Asian Journal of Chemistry; Vol. 35, No. 2 (2023), 422-430

ASIAN JOURNAL OF CHEMISTRY

https://doi.org/10.14233/ajchem.2023.26881

Suitability of ZnO Nanocomposite of Copolymer (PPy-PNVK-ZnO) (PPy = Polypyrrole; PNVK = Poly 9-vinyl carbazole) for the Detection of 6-Thioguanine: A DFT Analysis

KIRTESH PRATAP KHARE[1,2,*], RACHANA KATHAL[1], NEELIMA SHUKLA[3], REENA SRIVASTAVA[2] and ANURAG SRIVASTAVA[2]

[1]Department of Chemistry, Amity School of Engineering & Technology, Amity University, Gwalior-474005, India
[2]Advance Materials Research Group and Materials Synthesis and Sensor Design Lab, ABV-Indian Institute of Information Technology and Management, Gwalior-474015, India
[3]Department of Chemistry, Srimant Madhavrao Scindia Government Model Science College, Gwalior-474009, India

*Corresponding author: E-mail: kirteshkhare01@gmail.com

Received: 23 October 2022; *Accepted*: 12 December 2022; *Published online*: 30 January 2023; AJC-21125

Conducting polymers have extensively been exploited for the specific drug detection, through diverse drug responses. 6-Thioguanine (6-TG) is commonly used in the treatment of cancer and its level monitoring in the human body is essential to avoid the side effects due to its physiological metabolites. Computational synthesis of a novel sensor material, *i.e.* ZnO nanocomposite of copolymer (PPy-PNVK-ZnO) using polypyrrole (PPy-ZnO) and poly 9-vinyl carbazole (PNVK-ZnO) polymers, has been performed and investigated its sensing ability for 6-TG drug, using the density functional theory (DFT) based *ab initio* approach. Generalized gradient approximation (GGA), parameterized with Perdew, Burke and Ernzerhof (PBE) type parameterization furnishes novel resources on the studied molecular model. The molecular interactions have been analyzed in terms of the HOMO-LUMO gap, density of states (DOS), adsorption energy (E_{ads}), recovery time (τ), Mulliken population, electron density plot and quantum molecular descriptors. The calculated negative adsorption energy confirms the stability of these polymers and observes the type of interaction with 6-TG, as physical adsorption, that also confirms the reusability of the prepared sensor and its low operational temperature. It has also been observed that ZnO nanocomposite of copolymer has favourable stability in comparison to its host counterparts, whereas the host PNVK has a better recovery time and PPy has a relatively better range of detection and highly reactive.

Keywords: Density functional theory, Polymeric sensor, 6-Thioguanine, Anticancer drug, Electronic properties, Recovery time.

INTRODUCTION

6-Thioguanine (6-TG), a thiopurine and immunosuppressive drug is widely utilized in the treatment of cancer and anti-tumour [1-3]. When combined with human DNA, the physiologic route to oxidation and methylation of the exocyclic sulphur atom is taken up by 6-TG, leading to mismatches during replication, repair system activation, and ultimately cell-cycle disruption and cell death [2,4]. Wide application of 6-TG as an anticancer therapeutic agent for its detection such as high performance liquid chromatography [5], surface plasmon resonance [6] and electrodic analyses [7] have explored its metabolic pathways to study its mode of action and related mechanisms. Conventional analytical methods have exclusive installation and operational procedures as bottlenecks to the analyses applied. This necessitates the development of unpretentious and sensitive methods for the detection of 6-TG.

Since decades, conducting polymers have fascinated the researchers to develop electrodic devices for recognition and intensification of signals for redox analysis of the analyte in medical diagnosis, repetitive investigations on food and pharmaceuticals, environmental monitoring of trace metals, *etc.* [8]. The milestone analytical science of conducting polymer sensors as signal enhancing element in electroanalytical applications deserve attention [9]. Such polymers consist of a group of moieties (*viz.* polypyrrole, polyaniline, polythiophene and their derivatives) and have attracted considerable attention due to their lightweight, scalability, flexibility, appreciable thin layer forming property, semiconductivity, thermal and environmental stability, resistance to corrosion, *etc.* [10]. Conducting polymers can be specifically custom-made by the chemist for precise requirements rendering them alluring substitutes for explicit constituents used for the creation of various sensors.

The electrochemical sensors have marveled in the new age of sensing devices with conducting polymers and nanocarbon materials [11]. The modified interface imparts advantageous physical and chemical characteristics of the transformer [12] novel material [13] along with strong mechanical strength [14]. In recent years, various electrodic devices based on electroactive polymers have been developed for significant applications in electroanalytical and materials science to determine the diverse range of analytes [14]. Challenges with pure conducting polymers like low sensitivity, surface poisoning, poor selectivity, adsorption of reaction intermediates and interference with other species constituted few initial problems [15], facile synthesis, superior response and morphological varieties prove polymer nanocomposites (PNCs) as excellent transducers in electroanalytical sensors, in comparison with those obtained by their neat counterparts [16].

Nanoparticles in the polymer composites [17] bestow the latter with improved mechanical, photonic and electrical characteristics without compromising processability or weight [18]. Features of nanoparticles *viz.* the size to mass ratio, specific morphologies and altered physical and chemical properties provide multiple applications in the field of medicine, environment, agriculture and textile [19,20]. Metal oxide nanoparticles have received greater significance for being less toxic in nature [21,22]. Various efforts have been made on metal oxide-based nanocomposites [23]. Polypyrrole-platinum (PPy-Pt) nanocomposite fabricated voltammetric sensor reported H_2O_2 with appreciable detection limit [24]. Polyaniline-gold nanoparticles (PANI-AuNPs) nanocomposite impregnated on glassy carbon electrode has been testified for the concurrent quantification of epinephrine and uric acid [25]. Zinc oxide (ZnO) nanostructures furnish materials that may be tailored with various synthetic procedures resulting in nanowires [26], nanorods [27], nanobelts [28], nanorings [29] and nanocages [30]. Of late, ZnO has attracted the considerable attention of scientists [31].

DFT based computation has many advantages over other analytical methods like modest operation, quick results, low cost and less time consumption for trace analyses. Few studies [32,33] are available on DFT based computational methods using biosensor materials for the copolymerization and trace level detection of drugs. Herein, a new computationally synthesized ZnO nanocomposite of copolymer (PPy-PNVK-ZnO) in the presence of 6-thioguanine (6-TG) drug moiety using quantum ATK method is reported that has been analyzed through stability analysis, HOMO-LUMO gap, electronic properties, charge transfer analysis and compared with host polymers (PPy-ZnO and PNVK-ZnO).

COMPUTATIONAL METHODS

To analyze the sensing behaviour of ZnO nanocomposite of polypyrrole (PPy), poly 9-vinyl carbazole (PNVK) and their copolymer towards 6-thioguanine (6-TG), calculations have been performed using density functional theory (DFT) [34] based *ab initio* approach through Quantum ATK method [35]. Quantum ATK is an extended version of TranSIESTA. Projected assembly, along with its electronic and transference characteristics, has been computed using generalized gradient approximation (GGA), with Perdew-Burke-Ernzerhof (PBE) [36] type parameterization. All the electronic states have been estimated using Double zeta double polarized (DZDP) basis sets. The energy spectrum has been calculated using 1 × 1 × 1 k-point sampling. A mesh cut-off of 75 Rydberg has been used for the amplified electron density on a systematic real-space grid. Optimization has been accomplished by periodically relaxing the cell constriction. Different possible configurations have been optimized to confirm the structural stability of ZnO nanocomposite of PPy, PNVK and their copolymer in the presence of 6-TG. For optimization of geometries, the maximum stress tolerance has been set to 0.05 eV/Å^3 with a maximum force of 0.05 eV/Å, respectively. The ZnO nanocomposite of PPy containing 8 carbon atoms, 2 nitrogen atoms, 8 hydrogen atoms, 1 zinc atom and 1 oxygen atom and PNVK containing 28 carbon atoms, 2 nitrogen atoms, 20 hydrogen atoms, 1 zinc atom and 1 oxygen atom has been considered as the host materials for the polymeric drug sensor and to further design a new conducting copolymer to understand its sensing ability for 6-TG.

RESULTS AND DISCUSSION

Structural stability analysis: The optimized spatial patterns of ZnO nanocomposite of (Fig. 1b,c) PPy, (Fig. 1d,e) PNVK and their (Fig. 1f,g) copolymer as conducting material in the presence/absence of 6-thioguanine (6-TG) are shown in Fig. 1. As the number of atoms increases in the ZnO nanocomposite of copolymer compared to polypyrrole (PPy) and poly 9-vinyl carbazole (PNVK) host polymers, the surface-to-volume ratio also increases. The ZnO nanocomposite of PPy, PNVK and their copolymer based sensing materials should be established before launching the adsorption process of 6-TG for cancer treatment. The computed total energy of ZnO nanocomposite of copolymer and host polymers decreases with the increasing number of atoms. The computed total energy observes a trend ZnO nanocomposite of PPy > PNVK > copolymer in the presence/absence of 6-TG and stability just reverse with the total energy. Results furnish that PPy < PNVK < copolymer trend for stability and approve more stability of ZnO nanocomposite of copolymer in the presence/absence of 6-TG, in comparison to ZnO nanocomposite of PPy and PNVK host polymers (Table-1).

TABLE-1
TOTAL ENERGY OF ZnO NANOCOMPOSITE OF PPy, PNVK AND THEIR COPOLYMER

System	Total energy (eV)
PPy-ZnO	-3905.21
PNVK-ZnO	-7242.53
Copolymer_ZnO	-9139.96
PPy-ZnO + 6 TG	-6487.33
PNVK-ZnO + 6 TG	-9824.97
Copolymer_ZnO + 6 TG	-11722.24

To understand the chemistry between adsorbate and adsorbent, the optimized geometries have been analyzed in terms of mode of interaction and bond parameters. In case of ZnO nanocomposite of (Fig. 1g) copolymer as well as host (Fig. 1c,e) polymers, in the presence of (Fig. 1a) 6-TG, the interaction is physical adsorption. During the interaction, the bond parameters,

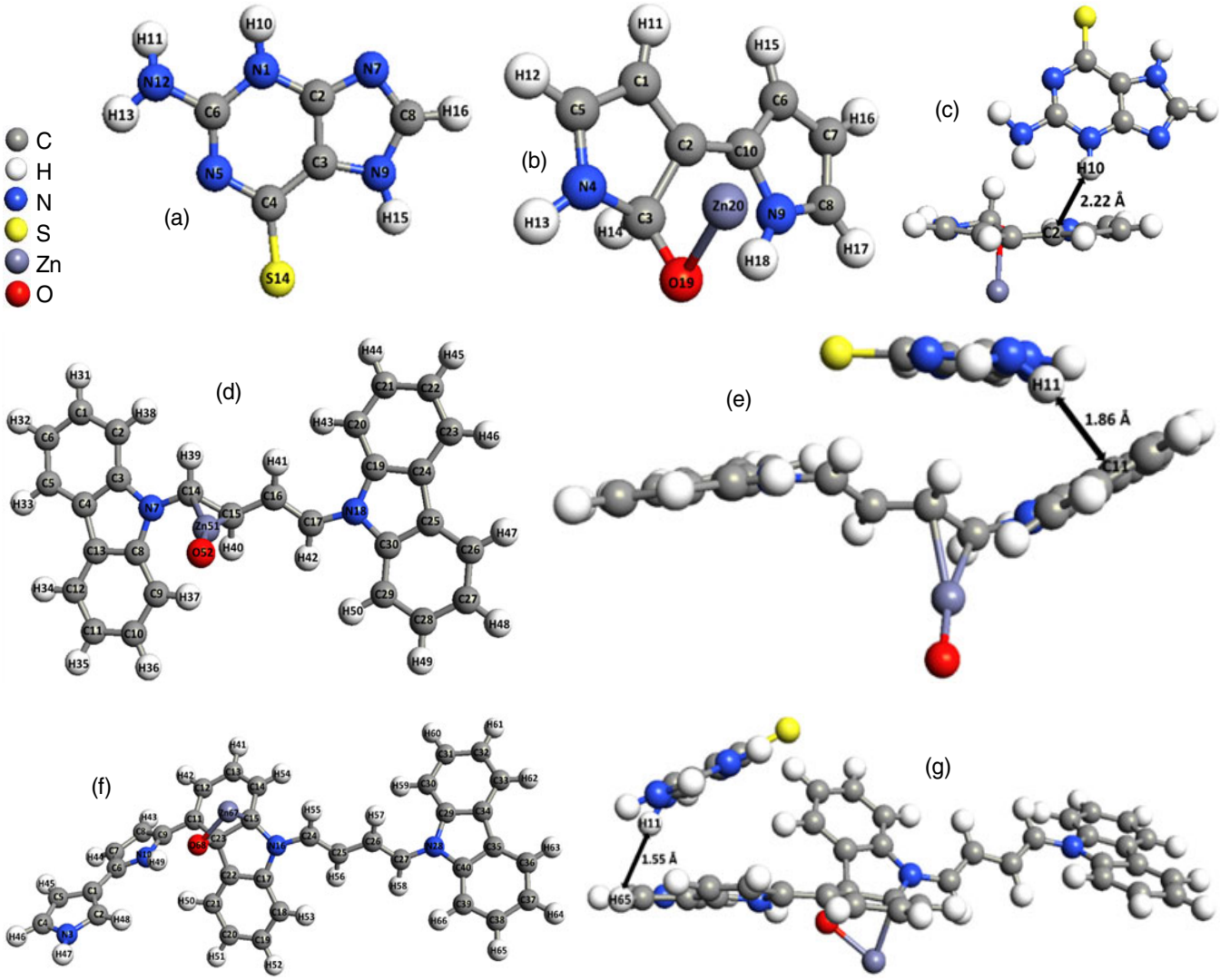

Fig. 1. Optimized geometries of ZnO nanocomposite of (b,c) PPy, (d,e) PNVK and their (f,g) copolymer in the presence/absence of (a) 6 TG

i.e. bond length and bond angle of 6-TG and ZnO nanocomposite of PPy, PNVK and their copolymer in the presence of 6-TG, found altered (Table-2). Higher electronegativity possessed by oxygen and nitrogen atoms seems to be responsible for the variation in the bond parameters. The oxygen atom of ZnO has highly affected the bond parameters in comparison to other atoms, the reason being oxygen atom contains two loan pair(s) and its higher electronegativity, than the other atoms and observes a trend zinc < hydrogen < carbon < sulfur < nitrogen < oxygen over Pauling scale 1.65, 2.20, 2.55, 2.58, 3.04 and 3.44, respectively.

Interestingly, during the interaction between adsorbate and adsorbent, the bond length and bond angle of ZnO nanocomposite of PPy, PNVK and their copolymer is affected due to the presence of 6-TG (Table-2). In case of ZnO nanocomposite of PNVK, the bond length and bond angle in the presence of 6-TG, highly varied between Zn_{51}-C_{15} and O_{52}-Zn_{51}-C_{15} atoms, in comparison to PPy and copolymer and the value is 0.08 Å and 9.05º, respectively. Similarly, the bond length and angle have also been computed for the affected orientation of 6-TG for ZnO nanocomposite of PPy, PVNK and their copolymer. The bond length of 6-TG between N_1-H_{10} atoms has highly got changed with ZnO nanocomposite of PPy, with the value 0.02 Å. However, the bond angle of 6-TG highly got altered with ZnO nanocomposite of copolymer between H_{10}-N_1-C_2 atoms, with the value 2.17º.

To understand the type of interaction between adsorbate and adsorbent, the adsorption energy (E_{ads}) of the interaction has been computed using eqn. 1:

$$E_{ads} = E_{T(X + 6\text{-}TG)} - E_{T(X)} - E_{T(6\text{-}TG)} \quad (1)$$

where, $E_{T(X + 6\text{-}TG)}$ is the total energy of the optimized system, $E_{T(X)}$ is the total energy of ZnO nanocomposite of PPy, PNVK and their copolymer and $E_{T(6\text{-}TG)}$ is the total energy of optimized 6-TG. In eqn. 1, X corresponds to the ZnO nanocomposite of PPy, PNVK and copolymer, respectively. The negative value of E_{ads} (Table-3) confirms the physisorption and exothermic interaction between the adsorbate and adsorbent, indicating the adsorption system as stable due to weak van der Waal's forces. The ZnO nanocomposite of PNVK exhibits relatively weaker physical adsorption, followed by copolymer and PPy, as inferred from their lower and higher magnitudes of adsorption energies, respectively. It is interesting to observe that the E_{ads}

TABLE-2
BOND PARAMETERS OF ZnO NANOCOMPOSITE OF PPy, PNVK AND THEIR COPOLYMER IN THE PRESENCE OF 6 TG

System	Interacting atoms	Optimized bond length (Å)	Optimized bond angle (°)
6 TG	C_2-N_7	1.36	
	C_2-N_1	1.37	
	N_1-H_{10}	**1.03**	
	N_1-C_6	1.37	
	$\angle H_{11}$-N_{12}-H_{13}		114.13
	$\angle H_{13}$-N_{12}-C_6		111.15
	$\angle H_{11}$-N_{12}-C_6		117.25
	$\angle N_{12}$-C_6-N_5		117.79
	$\angle C_6$-N_1-H_{10}		122.98
PPy-ZnO	O_{19}-Zn_{20}	2.12	
	C_2-C_{10}	1.45	
	C_7-C_8	1.39	
	$\angle Zn_{20}$-O_{19}-C_3		83.18
	$\angle N_4$-C_3-C_2		98.17
	$\angle O_{19}$-C_3-C_2		116.98
	$\angle C_3$-C_2-C_{10}		116.06
	$\angle C_{10}$-N_9-C_8		110.27
	$\angle H_{18}$-N_9-C_8		131.22
	$\angle H_{16}$-C_7-C_8		124.96
	$\angle C_7$-C_8-H_{17}		129.88
	$\angle C_8$-N_9-H_{18}		131.22
	$\angle C_8$-N_9-C_{10}		110.27
6 TG	N_{12}-C_6	1.37	
	N_1-H_{10}	1.02	
	N_1-C_2	1.37	
	C_4-S_{14}	1.67	
	N_5-C_4	1.38	
	N_5-C_6	1.32	
	$\angle H_{11}$-N_{12}-C_6		115.77
	$\angle N_5$-C_4-S_{14}		124.46
	$\angle C_2$-C_3-C_4		123.79
	$\angle N_7$-C_2-C_3		112.94
	$\angle C_4$-C_3-N_9		132.18
	$\angle C_3$-N_9-C_8		106.97
	$\angle C_2$-C_3-N_9		103.98
PNVK-ZnO	N_7-C_3	1.39	
	C_2-H_{38}	1.09	
	C_8-N_7	1.39	
	C_9-H_{37}	1.10	
	C_{11}-H_{35}	1.10	
	C_{11}-C_{12}	1.40	
	C_{14}-Zn_{51}	2.07	
	Zn_{51}-C_{15}	**2.21**	
	$\angle C_{14}$-N_7-C_8		126.97
	$\angle N_7$-C_{14}-Zn_{51}		114.63
	$\angle H_{39}$-C_{14}-Zn_{51}		107.36
	$\angle C_{14}$-Zn_{51}-O_{52}		167.05
	$\angle O_{52}$-Zn_{51}-C_{15}		**151.44**
	$\angle Zn_{51}$-C_{15}-H_{40}		105.50
	$\angle C_{17}$-N_{18}-C_{19}		127.81
6 TG	N_7-C_2	1.36	
	N_5-C_6	1.32	
	$\angle H_{11}$-N_{12}-H_{13}		112.56
	$\angle H_{13}$-N_{12}-C_6		109.60
	$\angle H_{11}$-N_{12}-C_6		114.57
	$\angle C_6$-N_1-C_2		117.10
	$\angle H_{10}$-N_1-C_2		**121.13**
	$\angle N_5$-C_4-S_{14}		124.71
	$\angle C_4$-C_3-C_2		123.84
	$\angle C_4$-C_3-N_9		132.12
	$\angle H_{15}$-N_9-C_8		130.99
Copolymer_ZnO	C_{32}-C_{33}	1.39	
	N_{38}-C_{39}	1.40	
	$\angle C_5$-C_1-C_6		127.49
	$\angle Zn_{67}$-C_{15}-C_{14}		113.38
	$\angle H_{51}$-C_{19}-C_{20}		121.58

TABLE-3
ADSORPTION ENERGY OF ZnO NANOCOMPOSITE OF PPy, PNVK AND THEIR COPOLYMER

System	Adsorption energy (eV)	Type of interaction
PPy-ZnO + 6 TG	-0.63	Physisorption
PNVK-ZnO + 6 TG	-0.94	Physisorption
Copolymer_ZnO + 6 TG	-0.78	Physisorption

of 6-TG adsorbed ZnO nanocomposite PPy, PNVK and their copolymer are proportional to their electronegativity. Thus, ZnO nanocomposite of PPy possess the highest E_{ads} despite having large adsorption distance, whereas the lowest adsorption distance has been observed for copolymer (Table-4) [37]. To support the inference of physical adsorption, the mode of interaction has also been verified through optimized structural geometries and electron density plots, as shown in Fig. 1c,e,g and Fig. 2c,e,g, respectively, which indicate that no chemical bond formed between the ZnO nanocomposite of PPy, PNVK and their copolymer with 6-TG.

TABLE-4
DISTANCE (RANGE OF DETECTION), HOMO-LUMO GAP AND CHARGE TRANSFER PROFILES BETWEEN ZnO NANOCOMPOSITE OF PPy, PNVK AND THEIR COPOLYMER WITH 6 TG

System	Optimized distance (Å)	HOMO-LUMO gap (eV)	Q_T (e)
PPy-ZnO + 6 TG	2.22	0.68	0.083
PNVK-ZnO + 6 TG	1.86	0.90	-0.037
Copolymer_ZnO + 6 TG	1.55	0.84	-0.017

For a quality sensor, its detection range is also an important parameter. Hence, the detection range has also been computed for these three interactions (Fig. 1c,e,g). The ZnO nanocomposite of PPy has a relatively larger detection range and, hence, better sensing ability than copolymer and PNVK. The optimized distance in the ZnO nanocomposite of PNVK with 6-TG system is 1.86 Å, followed by the copolymer at 1.55 Å and PPy at 2.22 Å (Table-4). The variation in range of detection can be attributed to the geometry of 6-TG, as well as the repulsions between the

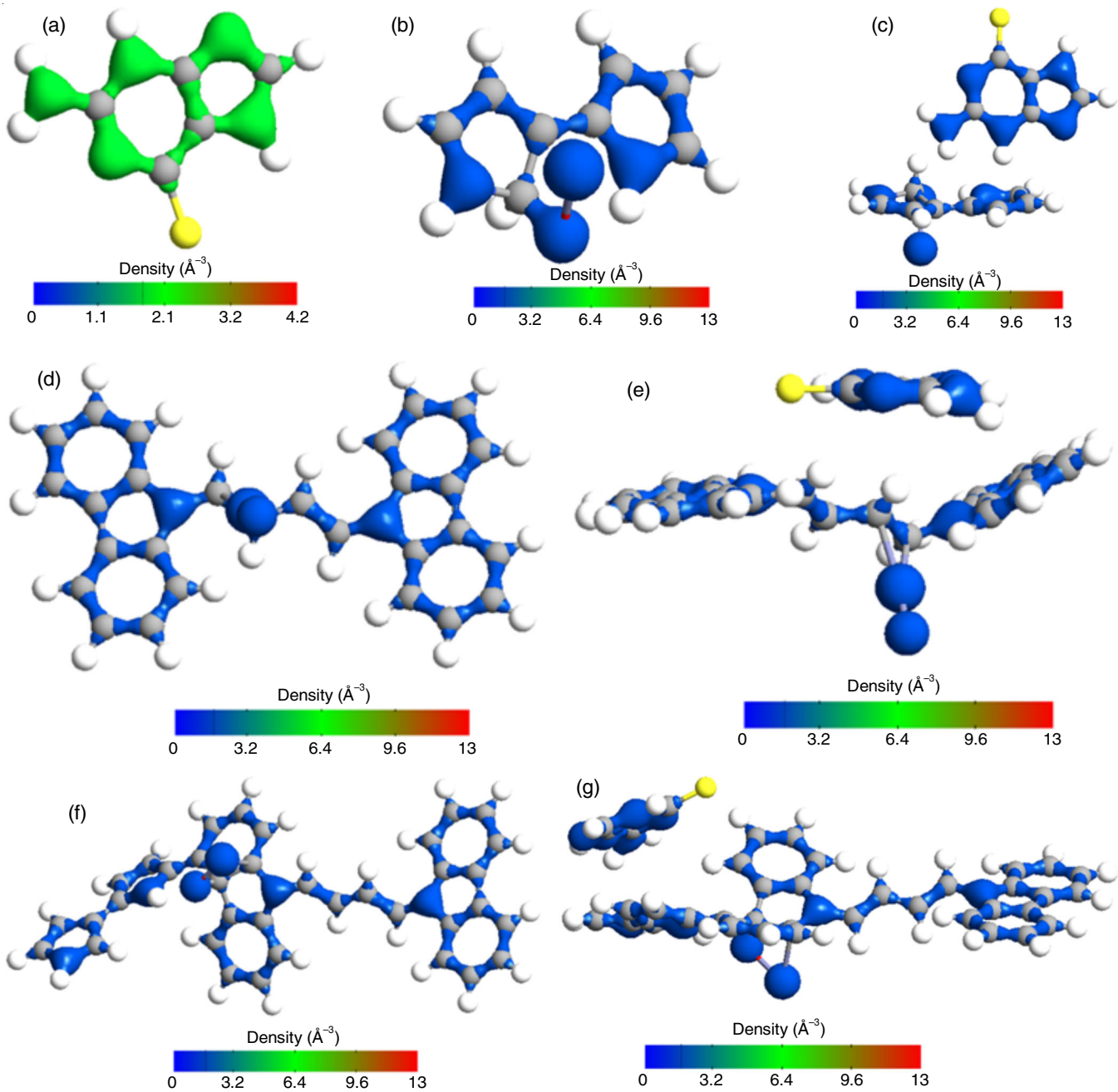

Fig. 2. Electron density plot (at an isovalue = 1.75094) of ZnO nanocomposite of (b,c) PPy, (d,e) PNVK and their (f,g) copolymer in the presence/absence of (a) 6 TG

delocalized electrons and loan pair(s) of ZnO nanocomposite of PPy, PNVK and their copolymer.

Recovery time (τ), yet another essential sensing parameter, has been computed using eqn. 2 [38]:

$$\tau = \nu^{-1} \exp\left(-\frac{E_{ads}}{K_b T}\right) \quad (2)$$

where, ν is the attempt frequency, K_b the Boltzmann constant and T operational temperature of the sensor. The calculated E_{ads} for 6-TG adsorbed ZnO nanocomposite of PPy, PNVK and their copolymer are found negative (Table-3, negative E_{ads} represent the interaction is exothermic) and the adsorption energy has an inverse relationship with its recovery time. The computed E_{ads} observes a trend ZnO nanocomposite of PPy > copolymer > PNVK and recovery time just reverse with E_{ads}. Results conformed that PPy < copolymer < PNVK trend for recovery time and approve fast recovery time of ZnO nanocomposite of PNVK at low operational temperature for 6-TG sensing, in comparison to PPy and copolymer (Table-3). The sensitivity of 6-TG at different orientations on ZnO nanocomposite of PPy, PNVK and their copolymer has also been analyzed.

Charge transfer analysis: To measure the interaction intensity between adsorbate and adsorbent, the charge transfer analysis has also been performed by the Mulliken population analysis, using eqn. 3 and also confirmed by the electron density plot.

$$\Delta\rho = \rho_{(X + 6\text{-TG})} - \rho_{(6\text{-TG})} \quad (3)$$

where, $\rho_{(X + 6\text{-TG})}$ is the charge on 6-TG of adsorbed system and $\rho_{(6\ TG)}$ is the charge on 6-TG. In eqn. 3, X corresponds to the ZnO nanocomposite of PPy, PNVK and copolymer, respectively. The positive value of charge transfer indicates the transfer of charge from adsorbent to adsorbate and the negative value indicates the charge transfer from adsorbate to the adsorbent. In case of ZnO nanocomposite of PPy, the charge transfer occurrence from PPy to 6-TG is observed, whereas in case of PNVK and copolymer, the charge transfer incidents from 6-TG to PNVK and copolymer, illustrates a weak binding between the adsorbent and the adsorbate and hence supports the physisorption reaction exist between the adsorbate and adsorbent. The amount of charge transfer in case of ZnO nanocomposite of PPy (0.083) is relatively higher in comparison to the PNVK (-0.037) and copolymer (-0.017) (Table-4).

The computed charge transfer results from interactions between adsorbate and adsorbent and the same has been shown through the electron density plots of the adsorbed systems (Fig. 2a-g). It has been observed that the ZnO nanocomposite of PPy, donate charge to 6-TG. On the other hand, PNVK and copolymer gain charge from 6-TG, as confirmed by dark blue colour over the PPy, PNVK and their copolymer. Overall, there is no evidence of chemisorption between adsorbate and adsorbent and the value of charge transfer further supports the physisorption type interaction.

Electronic properties: The variation in the electronic properties of ZnO nanocomposite of PPy, PNVK and their copolymer on the adsorption of 6-TG is analyzed, in terms of MES plots, HOMO-LUMO gap and DOS profiles (Fig. 3a-c). It is well known fact that the electrical conductivity of materials can be control through the bandgap of the material, computed through ~ $\exp(-E_g/K_BT)$ [39]; where, E_g is the bandgap of material, K_B is the Boltzmann constant and T is the absolute temperature. The HOMO-LUMO gap, similar to the bandgap for polymers materials, is indicated in the DOS profiles (Fig. 3a-c) for all the adsorbed systems.

The electronic nature of ZnO nanocomposite of PPy, PNVK and their copolymer in the presence/absence of 6-TG has been estimated through the MES profiles plotted in Fig. 3a-c. The MES plot indicates a computed HOMO-LUMO gap of ZnO nanocomposite of PPy, PNVK and their copolymer is 1.32 eV, 1 eV and 0.88 eV, repectively in the absence of 6-TG and reduces to 0.68 eV, 0.9 eV and 0.84 eV, respectively, in the presence of 6-TG, shown in left panel of Fig. 3a-c. The MES plots indicating the enhanced conducting ability of ZnO nanocomposite of PPy, PNVK and their copolymer after adsorption of 6-TG. Thus, the ZnO nanocomposite of PPy possess better conducting ability towards 6-TG in comparison to PNVK and copolymer.

Furthermore, the DOS profiles have also been computed to understand the impact of 6-TG on ZnO nanocomposite of PPy, PNVK and their copolymer. The DOS profiles of PPy, PNVK and their copolymer in the presence of 6-TG indicate that the HOMO-LUMO gap get reduced by 48.48%, 10% and 4.54%, respectively. It is enough to mention that the variation in DOS profiles of the adsorbed system is in line with their computed MES profiles. From the DOS profiles, the peaks of HOMO and LUMO get shifted towards the Fermi level, in all the adsorbed systems and resulting in variation of the HOMO-LUMO gap as shown in the right panel of Fig. 3a-c. In case of ZnO nanocomposite of PPy (Fig. 3a) in the presence of 6-TG, one extra peak appears in the conduction band and the height of few peaks varies in the valence band. In case of ZnO nanocomposite of PNVK (Fig. 3b), due to the presence of 6-TG, few extra peaks appear and the height of few peaks varies in the valance/conduction band. Whereas, in case of ZnO nanocomposite of copolymer (Fig. 3c) in the presence of 6-TG, a reduction in few peaks have been observed and the height of few peaks varies in valance/conduction band.

The variation in the HOMO-LUMO gap as a function of detection range for all the adsorbed systems are shown in Fig. 4. Where, it is observed that the HOMO-LUMO gap, continuously decreases and that may be attributed to the enhanced conductance in the adsorbed systems. These findings further confirms the sensing of 6-TG through the ZnO nanocomposite of PPy, PNVK and their copolymer. The best range of detection has been observed in the ZnO nanocomposite of PPy.

Quantum molecular descriptors: In order to further understand the reactivity of ZnO nanocomposite of PPy, PNVK and their copolymer with 6-TG; softness ($S = 1/\eta$) and global hardness ($\eta = (E_{LUMO}-E_{HOMO})/2$) have been calculated using Koopman theorem [40]; where, the value of S is minimum for 6-TG adsorbed ZnO nanocomposite of PPy. The softness of 6-TG adsorbed ZnO nanocomposite of PPy is also verified through the hardness due to the inverse relationship between them. The η is indicative of resistance towards electron cloud change of the chemical system. The value of η for ZnO nanocomposite of PPy decreases upon adsorption of 6-TG (Table-5). Hence, the hardness and HOMO-LUMO gap of the molecule are associated with reactivity; the less value of hardness and lower value of the HOMO-LUMO gap indicates that the molecule is highly reactive. An electronic system with a larger HOMO-LUMO gap should be less reactive than one having smaller gap [41,42]. The η corresponds to the gap between the HOMO and LUMO orbital energies. The larger the HOMO-LUMO orbital energy gap, the harder the molecule. The hardness has been associated with the stability of the chemical system. It has been observed that 6-TG adsorbed ZnO nanocomposite of PPy is relatively better in terms of sensing and increases the chemical reactivity in comparison to the ZnO nanocomposite of PNVK and copolymer.

TABLE-5
CALCULATED ENERGIES OF FRONTIER MOLECULAR ORBITALS (E_{HOMO}, E_{LUMO}), SOFTNESS (S) AND GLOBAL HARDNESS (η) OF SYSTEMS

System	E_{HOMO} (eV)	E_{LUMO} (eV)	S (eV)	η (eV)
PPy-ZnO	-0.66	0.66	1.51	0.66
PNVK-ZnO	-0.50	0.50	2.00	0.50
Copolymer_ZnO	-0.44	0.44	2.27	0.44
PPy-ZnO + 6 TG	-0.34	0.34	2.94	0.34
PNVK-ZnO + 6 TG	-0.45	0.45	2.22	0.45
Copolymer_ZnO + 6 TG	-0.42	0.42	2.38	0.42

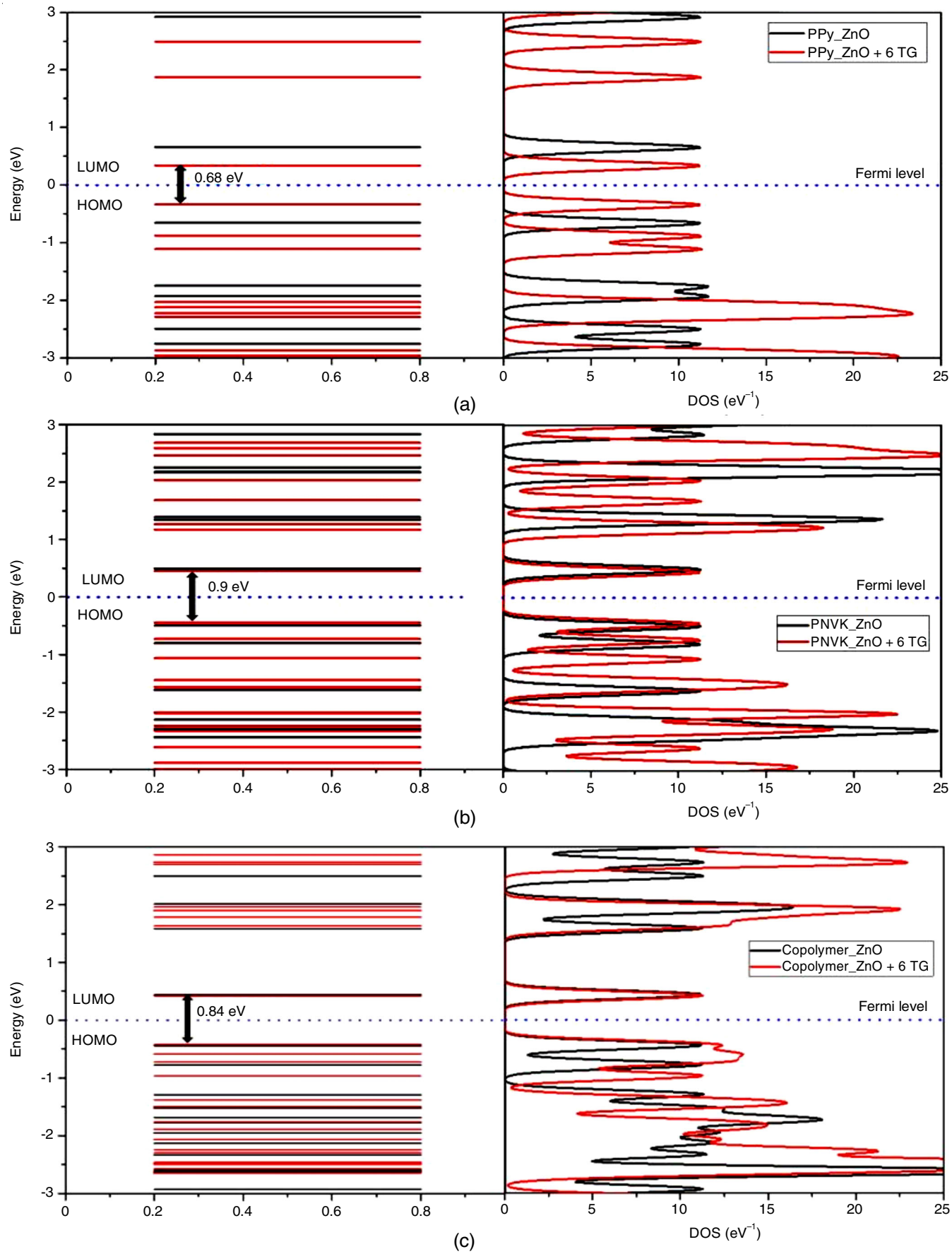

Fig. 3. HOMO-LUMO gap and DOS profile of ZnO nanocomposite of (a) PPy, (b) PNVK and their (c) copolymer in the presence/absence of 6 TG

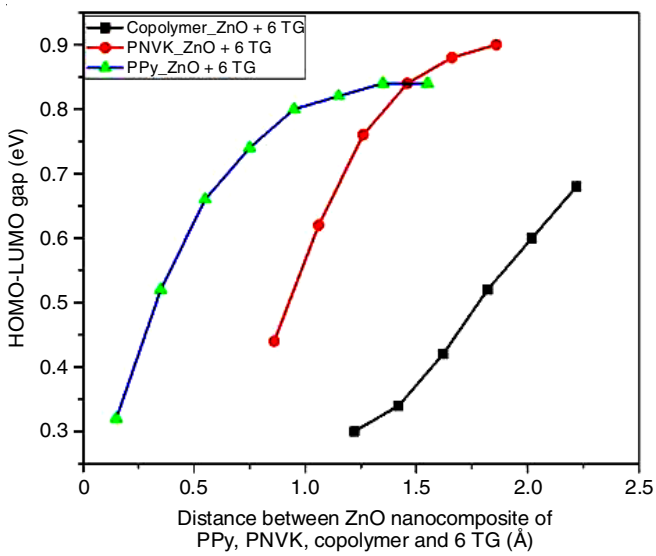

Fig. 4. HOMO-LUMO gap as a function of the distance between ZnO nanocomposite of PPy, PNVK and their copolymer with 6 TG

Conclusion

The present study reports the simulation on the adsorption activity of computationally synthesized ZnO nanocomposite of copolymer (PPy-PNVK) and host polymers (PPy and PNVK), with an objective to assess the suitability of these polymers as a polymeric sensor for 6-thioguanine (6-TG). The DOS profile, MES profile, HOMO-LUMO gap, adsorption energy, recovery time, Mulliken population, electron density plots have been analyzed for the proposed polymeric sensor to detect 6-TG drug. The significant variations in the electronic properties and quantum molecular descriptors of ZnO nanocomposite of the copolymer and host polymers confirmed the sensing of 6-TG. The results show that ZnO nanocomposite of copolymer shows better stability towards 6-TG than host polymers. The physical adsorption of 6-TG on copolymer and host polymers confirms the reusability of the device formed using these synthesized materials with low operational temperature. The ZnO nanocomposite of PNVK has a better recovery time, whereas the PPy has a relatively better range of detection and is highly reactive. As these results are based on computational modeling and are being reported for the very first time, certainly, may trigger a good number of researchers interested in cancer treatment and these polymer based systems.

ACKNOWLEDGEMENTS

The authors put on record their heartfelt appreciation to Advanced Materials Research Group (AMRG) of Materials synthesis and sensor designing Lab at Atal Bihari Vajpayee Indian Institute of Information Technology and Management, Gwalior (ABV-IIITM) for providing the computational resources for the research work.

CONFLICT OF INTEREST

The authors declare that there is no conflict of interests regarding the publication of this article.

REFERENCES

1. B. Meijer, C.J.J. Mulder, G.J. Peters, A.A. van Bodegraven and N.K.H. de Boer, *World J. Gastroenterol.*, **22**, 9012 (2016); https://doi.org/10.3748/wjg.v22.i40.9012
2. P. Karran, *Br. Med. Bull.*, **79-80**, 153 (2006); https://doi.org/10.1093/bmb/ldl020
3. P. Karran and N. Attard, *Nat. Rev. Cancer*, **8**, 24 (2008); https://doi.org/10.1038/nrc2292
4. E. Petit, S. Langouet, H. Akhdar, C. Nicolas-Nicolaz, A. Guillouzo and F. Morel, *Toxicol. In Vitro*, **22**, 632 (2008); https://doi.org/10.1016/j.tiv.2007.12.004
5. C.W. Keuzenkamp-Jansen, R.A. De Abreu, J.P.M. Bökkerink and J.M.F. Trijbels, *J. Chromatogr. B Biomed. Sci. Appl.*, **672**, 53 (1995); https://doi.org/10.1016/0378-4347(95)00206-X
6. N. Bi, M. Hu, H. Zhu, H. Qi, Y. Tian and H. Zhang, *Spectrochim. Acta A Mol. Biomol. Spectrosc.*, **107**, 24 (2013); https://doi.org/10.1016/j.saa.2013.01.014
7. W. Wang, S.-F. Wang and F. Xie, *Sens. Actuators B Chem.*, **120**, 238 (2006); https://doi.org/10.1016/j.snb.2006.02.012
8. L.G. Shaidarova and G.K. Budnikov, *J. Anal. Chem.*, **63**, 922 (2008); https://doi.org/10.1134/S106193480810002X
9. H. Shirakawa, E.J. Louis, A.G. MacDiarmid, C.K. Chiang and A.J. Heeger, *J. Chem. Soc. Chem. Commun.*, 578 (1977); https://doi.org/10.1039/c39770000578
10. N. Ka and C.S. Rout, *RSC Adv.*, **11**, 5659 (2021); https://doi.org/10.1039/D0RA07800J
11. T. Guinovart, M. Parrilla, G.A. Crespo, F.X. Rius and F.J. Andrade, *Analyst*, **138**, 5208 (2013); https://doi.org/10.1039/c3an00710c
12. D.S. Ghosh, I. Calizo, D. Teweldebrhan, E.P. Pokatilov, D.L. Nika, A.A. Balandin, W. Bao, F. Miao and C.N. Lau, *Appl. Phys. Lett.*, **92**, 151911 (2008); https://doi.org/10.1063/1.2907977
13. C.-Y. Lin, A. Balamurugan, Y.-H. Lai and K.-C. Ho, *Talanta*, **82**, 1905 (2010); https://doi.org/10.1016/j.talanta.2010.08.010
14. T. Wang, M. Farajollahi, Y.S. Choi, I-T. Lin, J.E. Marshall, N.M. Thompson, S. Kar-Narayan, J.D.W. Madden and S.K. Smoukov, *Interface Focus*, **6**, 20160026 (2016); http://doi.org/10.1098/rsfs.2016.0026
15. S. Prakash, T. Chakrabarty, A.K. Singh and V.K. Shahi, *Biosens. Bioelectron.*, **41**, 43 (2013); https://doi.org/10.1016/j.bios.2012.09.031
16. G.G. Wallace, M. Smyth and H. Zhao, *TrAC-Trends Analyt. Chem.*, **18**, 245 (1999); https://doi.org/10.1016/S0165-9936(98)00113-7
17. Y. Wang, A. Liu, Y. Han and T. Li, *Polym. Int.*, **69**, 7 (2020); https://doi.org/10.1002/pi.5907
18. O. Domínguez-Renedo, M.A. Alonso-Lomillo and M.J. Arcos-Martínez, *Crit. Rev. Environ. Sci. Technol.*, **43**, 1042 (2013); https://doi.org/10.1080/10934529.2011.627034
19. T.I. Shaheen, M.E. El-Naggar, J.S. Hussein, M. El-Bana, E. Emara, Z. El-Khayat, M.M.G. Fouda, H. Ebaid and A. Hebeish, *Biomed. Pharmacother.*, **83**, 865 (2016); https://doi.org/10.1016/j.biopha.2016.07.052
20. A. Saxena, R.M. Tripathi and R.P. Singh, *Dig. J. Nanomater. Biostruct.*, **5**, 427 (2010).
21. S. Lin, Y. Zhao, T. Xia, H. Meng, Z. Ji, R. Liu, S. George, S. Xiong, X. Wang, H. Zhang, S. Pokhrel, L. Mädler, R. Damoiseaux, S. Lin and A.E. Nel, *ACS Nano*, **5**, 7284 (2011); https://doi.org/10.1021/nn202116p
22. U.T. Khatoon, K. Mohan Mantravadi and G.V.S. Nageswara Rao, *Mater. Sci. Technol.*, **34**, 2214 (2018); https://doi.org/10.1080/02670836.2018.1482600
23. M.R. Mahmoudian, Y. Alias, W.J. Basirun and M. Ebadi, *Electrochim. Acta*, **72**, 46 (2012); https://doi.org/10.1016/j.electacta.2012.03.144
24. L. Xing, Q. Rong and Z. Ma, *Sens. Actuators B Chem.*, **221**, 242 (2015); https://doi.org/10.1016/j.snb.2015.06.078

25. L. Zou, Y. Li, S. Cao and B. Ye, *Talanta*, **117**, 333 (2013); https://doi.org/10.1016/j.talanta.2013.09.035
26. L.E. Greene, M. Law, D.H. Tan, M. Montano, J. Goldberger, G. Somorjai and P. Yang, *Nano Lett.*, **5**, 1231 (2005); https://doi.org/10.1021/nl050788p
27. B. Postels, M. Kreye, H.-H. Wehmann, A. Bakin, N. Boukos, A. Travlos and A. Waag, *Superlattices Microstruct.*, **42**, 425 (2007); https://doi.org/10.1016/j.spmi.2007.04.045
28. Z.W. Pan, Z.R. Dai and Z.L. Wang, *Science*, **291**, 1947 (2001); https://doi.org/10.1126/science.1058120
29. X.Y. Kong, Y. Ding, R. Yang and Z.L. Wang, *Science*, **303**, 1348 (2004); https://doi.org/10.1126/science.1092356
30. P.X. Gao and Z.L. Wang, *J. Am. Chem. Soc.*, **125**, 11299 (2003); https://doi.org/10.1021/ja035569p
31. H.A. Wahab, A.A. Salama, A.A. El Saeid, M. Willander, O. Nur and I.K. Battisha, *Results Phys.*, **9**, 809 (2018); https://doi.org/10.1016/j.rinp.2018.02.077
32. K.P. Khare, R. Kathal, N. Shukla, R. Srivastava and A. Srivastava, *AIP Conf. Proc.*, **2352**, 020072 (2021); https://doi.org/10.1063/5.0052388
33. K.P. Khare, R. Kathal and R. Srivastava, *Mater. Today Proc.*, **48**, 641 (2021); https://doi.org/10.1016/j.matpr.2021.06.040
34. W. Koch and M.C. Holthausen, A Chemist's Guide to Density Functional Theory, John Wiley & Sons (2015).
35. S. Smidstrup, T. Markussen, P. Vancraeyveld, J. Wellendorff, J. Schneider, T. Gunst, B. Verstichel, D. Stradi, P.A. Khomyakov, U.G. Vej-Hansen, M.-E. Lee, S.T. Chill, F. Rasmussen, G. Penazzi, F. Corsetti, A. Ojanperä, K. Jensen, M.L.N. Palsgaard, U. Martinez, A. Blom, M. Brandbyge and K. Stokbro, *J. Phys. Condens. Matter*, **32**, 15901 (2020); https://doi.org/10.1088/1361-648X/ab4007
36. X. Xu and W.A. Goddard III, *J. Chem. Phys.*, **121**, 4068 (2004); https://doi.org/10.1063/1.1771632
37. S. Gowtham, R.H. Scheicher, R. Ahuja, R. Pandey and S.P. Karna, *Phys. Rev. B Condens. Matter Mater. Phys.*, **76**, 33401 (2007); https://doi.org/10.1103/PhysRevB.76.033401
38. S. Agrawal, G. Kaushal and A. Srivastava, *Chem. Phys. Lett.*, **762**, 138121 (2021); https://doi.org/10.1016/j.cplett.2020.138121
39. K. Gaurav, B. SanthiBhushan, R. Mehla and A. Srivastava, *J. Electron. Mater.*, **50**, 1022 (2021); https://doi.org/10.1007/s11664-020-08663-0
40. J. Luo, Z.Q. Xue, W.M. Liu, J.L. Wu and Z.Q. Yang, *J. Phys. Chem. A*, **110**, 12005 (2006); https://doi.org/10.1021/jp063669m
41. R. Kurtaran, S. Odabasioglu, A. Azizoglu, H. Kara and O. Atakol, *Polyhedron*, **26**, 5069 (2007); https://doi.org/10.1016/j.poly.2007.07.021
42. M. Vatanparast and Z. Shariatinia, *J. Mol. Graph. Model.*, **89**, 50 (2019); https://doi.org/10.1016/j.jmgm.2019.02.012